GEOPHYSICAL RESEARCH LETTERS, VOL. ???, XXXX, DOI:10.1029/,

Evidence for the Chaotic Origin of Northern Annular Mode Variability

S. M. Osprey

National Centre for Atmospheric Science, Department of Physics, University of Oxford, United Kingdom

M. H. P. Ambaum

Department of Meteorology, University of Reading, United Kingdom

Correspondence to S. M. Osprey, Department of Physics, University of Oxford, United Kingdom (s.osprey@physics.ox.ac.uk)

Exponential spectra are found to characterize variability of the Northern Annular Mode (NAM) for periods less than 36 days. This corresponds to the observed rounding of the autocorrelation function at lags of a few days. The characteristic persistence timescales during winter and summer is found to be ∼5 days for these high frequencies. Beyond periods of 36 days the characteristic decorrelation timescale is ∼20 days during winter and ∼6 days in summer. We conclude that the NAM cannot be described by autoregressive models for high frequencies; the spectra are more consistent with low-order chaos. We also propose that the NAM exhibits regime behaviour, however the nature of this has yet to be identified.

1. Introduction

Identification of distinct modes of climate variability and their characterisitic timescales has been an active area of research. One particular example of this being the Northern Annular Mode (NAM) and its regional counterpart, the North Atlantic Oscillation (NAO). Previous studies of the NAO have recognised distinct behaviour over a range of timescales, prompting some to conclude that no one process can likely account for all variability [*Stephenson et al.*, 2000; *Keeley et al.*, 2009]. Previous studies link this variability to preferred states of the tropospheric jet following breaking of upper-level Rossby waves [*Woollings et al.*, 2008, 2010; *Hannachi*, 2010], while others link increased persistence times with the mean-latitude of the storm-tracks [*Barnes et al.*, 2010; *Barnes and Hartmann*, 2010]; an effect also recognised for the Southern Annular Mode [*Hartmann and Lo*, 1998]. *Gerber and Vallis* [2007], using an idealised model, found that the intraseasonal timescale of extratropical variability was not simply related to boundary layer friction or radiative timescales. They describe a feedback of the eddy-forcing on the jet which is sensitive to the longitudinal extent of the former: more pronounced localisation leads to reduced sensitivity of timescale to imposed friction and heating. In describing the NAM, other studies have recognised power-law characteristics for the low frequency spectra, providing evidence for a stochastic description [*Feldstein*, 2000; *Vallis et al.*, 2004; *Gerber and Vallis*, 2005; *Franzke and Woollings*, 2011].

Hasselmann [1976] provided the standard description of such noise processes in terms of a random walk (also called an AR1 process). In these processes the reddening of the spectrum is provided by memory processes which integrate the high-frequency noise.

These models can be generalised to higher order noise processes, including coloured noise (e.g., ARMA processes). Clearly such models would provide better fits to the data, as they have more fitting parameters, but generally lack physical justification. Consequently, we adopt the AR1 process as the archetypal noise model.

Exponential power-spectra have been identified in a number of idealised nonlinear systems and are thought to characterise low-dimensional chaos [*Sigeti and Horsthemke*, 1987; *Sigeti*, 1995b; *Ohtomo et al.*, 1995]. It is argued that these characteristics can help to differentiate deterministic low-order chaos from stochastic processes, whose power-spectra display power-law dependence [*Sigeti*, 1995a]. *Brandstater and Swinney* [1987] in annulus studies of Taylor-Couette flow, identified exponential spectra with intermittency: the transition from quasi-periodic to weakly turbulent regimes. Other examples include: non-periodic beating in heart rhythm studies [*Babloyantz and Destexhe*, 1988], the dynamics of flame fronts [*Elhamdi et al.*, 1993] and laboratory studies of plasmas [*Pace et al.*, 2008]. The slope of exponential spectra are thought to be largely independent of dynamics; the mathematical structure of associated timescales were explored in *Frisch and Morf* [1981].

Here we present evidence for an exponential form of the 1000 hPa NAM power-spectrum corresponding to periods of less than 36 days and conclude that this provides support for intermittent chaos controlling NAM behaviour for periods of several weeks, at least.

The paper briefly sets out describing the NAM timeseries used, before giving details of the sampling and methods used to construct time-of-year autocorrelations. We then show results of summer and winter NAM lag-autocorrelation and power-spectra, before finally

providing a motivating example of the spectral characteristics of low-dimensional chaos, using the Lorenz-63 system [*Lorenz*, 1963].

2. Data and Methods

Here we use NAM timeseries data for the period 1958–2001 as compiled for and outlined in *Baldwin and Dunkerton* [2001], and extended through to July 2006 (http://www.nwra.com/resumes/baldwin/nam.php). In summary, this comprises the principal component timeseries of the leading empirical orthogonal function (EOF) of deseasonalised zonal mean daily 1000 hPa geopotential height. The EOF is defined between 20°N–90°N, on 90-day smoothed timeseries between November-March. NAM anomalies were calculated by projecting the original deseasonalised timeseries onto the EOF.

A filter m is used to calculate the time-of-year lag-autocorrelation function $\rho(\tau; t')$, where t' is a particular time of year and τ is lag. The idealised filter is constructed following the convolution of a Gaussian of unit area (g) with a repeating Dirac-delta function (comb-filter); the latter being defined as,

$$\text{Ш}(t; t') \equiv \sum_{n=0}^{N-1} \delta(t - t' - Dn), \quad 0 < t' < D \tag{1}$$

centred on t', repeated every $D = 365$ days for N years. The Gaussian (g) is chosen with a standard deviation σ of 50 days, to achieve an adequate sampling within summer and winter, while maintaining a distinction between seasons. The filter is defined as,

$$m(t; t') = \int_{-\infty}^{\infty} g(u)\, \text{Ш}(t - u; t')\, du \doteq g * \text{Ш} \tag{2}$$

where, for future expedience, we introduce the convolution operator by way of an asterisk in the final term. Our measure for the *time-of-year* autocovariance $R(\tau;t')$ is found by correlating the unfiltered and filtered NAM time series, z,

$$R(\tau;t') = \int_{-\infty}^{\infty} m(t;t')\, z(t)\, z(t+\tau)\, dt \doteq m\, z \star\, z \tag{3}$$

Here we have defined the autocovariance operator using a star on the right of the equation. Associated with R is a local measure of the power spectrum for the daily NAM (P) which follows from the Wiener-Khintchine Thereom [*Wiener*, 1930; *Khintchine*, 1934]. This thereom states that the autocovariance function of a data series is equal to the inverse Fourier transform of the series' power spectrum. In the present context,

$$\begin{aligned} P(f;t') &= \mathcal{F}\left(R(\tau;t')\right) \\ &= (M * Z)\, Z^* \\ &= (G\, \text{Ш}_f * Z)\, Z^* \end{aligned} \tag{4}$$

where the upper-case parameters are the Fourier transforms of their lower-case equivalents, and where $\mathcal{F}$ represents the Fourier transform. A degree of symmetry is found between the masking function m and its Fourier transform M, i.e the Fourier transform of g (G) is itself a Gaussian, while Ш is associated with a similar sifting function in the frequency domain (Ш_f), with a discrete spacing of $1\,\text{year}^{-1}$. The masking function m and its transform M are shown in figure 1.

The influence of the masking function on P can be inferred from (1) and (4). In the limit as $D \to \infty$, $G\,\text{Ш}_f \to G$. This is tantamount to sampling the original data about *one*

region centred on t'. The convolution in (4) smooths power across a range of frequencies. For a red spectrum, power is redistributed from low to high frequencies, resulting in a *broadened* spectrum. This engenders a complimentary response in R, which can be understood from the Fourier *Reciprocity Principle*:

$$\Delta R \, \Delta P = 1 \tag{5}$$

which states that the characteristic timescale (autocorrelation-width) of the autocovariance function, ΔR, is equal to the inverse of the equivalent band-width of the power-spectrum, ΔP. Consequently, if sampling broadens the peak in P at low frequencies, there must be a corresponding sharpening in the autocovariance function R at small lag. This naturally explains results from previous studies showing reduced levels of autocorrelation in finite-length data [*Trenberth*, 1984].

For this study, we retrieve R for the 1000 hPa NAM by fitting a piecewise function to the power-spectrum, P, before inverting using (4). Firstly, we are guided to fit a Lorentzian to the low frequency part of P ($\omega < \omega_c$), as this corresponds to exponential decay at large lag in R, a characteristic of stochastic variability of an AR1 process, but is also linked with high dimensional chaos. We then fit an exponential function to high wavenumbers ($\omega \geq \omega_c$) as this characterises the presence of chaos in many low-dimensional systems. Specifically we do a least squares fit of P to:

$$P_{\text{fit}}(\omega; t') = \begin{cases} 2A\alpha(\alpha^2 + \omega^2)^{-1} & : \quad \omega < \omega_c \\ B \exp(-\beta\omega/2) & : \quad \omega \geq \omega_c \end{cases} \tag{6}$$

Here we identify A and B as the integrated power and α and β as characteristic frequency scales, for the low and high frequency fits, respectively. The cross-over frequency ω_c is chosen to minimise any discontinuity between the two retrieved fits. The autocovariance function is calculated from inverting (4), above. This supports our choice of minimising the misfit of $P_{\text{fit}}(\omega_c)$, as any significant discontinuity would introduce spurious numerical features following the inversion of (4). The time-of-year fitted autocorrelation function $\rho_{\text{fit}}(\tau; t')$ is defined as the ratio of the autocovariance function to its value at zero-lag,

$$\rho_{\text{fit}}(\tau; t') = R_{\text{fit}}(\tau; t')/R_{\text{fit}}(0; t') \tag{7}$$

Finally we define a width measure for the two portions of P_{fit} using equivalent width as described in *Bracewell* [1978], namely;

$$\Delta P_{\text{fit}} = \int_{-\infty}^{\infty} P_{\text{fit}}(f; t') d\tau / P_{\text{fit}}(0; t') \tag{8}$$

where we use values extrapolated over the *entire* frequency domain for each of the fits. Using (5), we can then calculate an autocorrelation timescale for low and high frequency portions of the spectra. We find that the autocorrelation timescales retrieved for low and high frequencies are $(1 - \alpha)^{-1}$ and $\beta\pi/4$, respectively. Uncertainity estimates (standard deviations) are calculated by varying ω_c within the range $5 < \omega_c < 15$ for winter and $20 < \omega_c < 40$ for summer.

3. Results

Figure 2 shows power spectra of the filtered summer and winter NAM time series on a semi-log scale. The winter period is centred on January 15 while the summer period

is centred on July 15. The results show little sensitivity to the precise specification of dates around mid-summer and mid-winter. Both spectra show broadband structure and enhanced power at low frequencies, with the wintertime NAM spectra exhibiting greater variance across all frequencies. The summertime spectrum exhibits a linear decrease in log-power at high frequencies ($\omega > \omega_c = 30 \times 2\pi\,\mathrm{year}^{-1}$), as shown on the semi-log scale, and is well described by an exponential whose corresponding autocorrelation width $\Delta\rho$ is (4.66 ± 0.04) days. At frequencies lower than ω_c, even though the spectral shape is Lorenzian, the retrieved timescale is (5.94 ± 0.05) days. The wintertime NAM spectra exhibits distinct structure at high and low frequencies. Frequencies greater than $\omega = 10 \times 2\pi\ \mathrm{yr}^{-1}$, equivalent to a period of 36 days, show a similar exponential relationship to those in summer, with a decay constant of (4.63 ± 0.04) days. At lower frequencies, the slope of the spectrum is steeper indicating a time scale of (20.64 ± 1.32) days.

Also shown in figure 2 are AR1 fits to the summer and winter spectra, computed over all frequencies. It is seen that although the fit is good over low frequencies during winter and low-mid frequencies during summer, it is generally poor elsewhere. At high frequencies the AR1 fit shallows, which is characteristic of power-law spectra, in stark contrast to the observed spectra and the exponential fits.

The summer and winter observed (ρ) and fitted (ρ_{fit}) NAM autocorrelations are shown in figure 3. The observed ρ for summer and winter shows a rounding off at lags less than than 2 days, and is consistent with day-to-day persistence, while the steeper slope at longer lag-times is associated with the breakdown of this persistence due to broadband natural variability. A noticeable reduction in the slope of the winter autocorrelation function is

seen beyond 6 days. This is directly linked with the piecewise structure found in the winter NAM spectra. This has been associated with a "shouldering" feature in previous studies, most noticeable near 20 days [*Ambaum and Hoskins*, 2002; *Norton*, 2003]. A similar feature is seen during summer at 20 days, although unlike winter, it is accompanied by a continued rapid decrease in the background.

4. Discussion and Conclusion

Power-law relationships describing the low frequency NAM variability can be found throughout the literature, though it is not apparent why such a description should be applicable at high frequencies. Arguments against this are outlined in *Sigeti and Horsthemke* [1987]. They reason that time series of deterministic systems can be differentiated to arbitrary order, unlike time series from stochastic processes. They state that the power-spectra of stochastic processes can only be described by a finite order power-law of the type ω^{-2n} ($n \in \mathcal{I}^+$) and so cannot decay at high frequency as fast as exponentially distributed spectra. The existence of an exponential relationship describing the summertime NAM and timescales shorter than $\sim$36 days during wintertime, suggests characteristics beyond simple power-law descriptions of underlying stochastic variability. *Sigeti* [1995b] show that the slope of an exponential spectrum (in our case ~ 5 days^{-1}) is proportional to the sum of the positive Lyapunov exponents (a defining characteristic of chaos), and thus related to the short term error growth of a dynamical system.

To explore the origins of the exponential characteristics of high-frequency NAM variability we examine the autocorrelation and spectral characteristics of the Lorenz-63 system – the classic example of a simple system exhibiting chaos [*Lorenz*, 1963]. We define the

following:

$$\begin{aligned} \dot{x} &= \sigma y - \sigma x \\ \dot{y} &= x(R - z) - y \\ \dot{z} &= xy - bz \end{aligned} \tag{9}$$

The values for the parameters are taken from *Lorenz* [1963], that is: $\sigma = 10.0$, $R = 28.0$ and $b = 8/3$. The equations were solved using a fourth-order Runga-Kutta scheme for 2000 model time units, sampled once every 0.1 time units.

Figure 4 shows a portion of the x-component time series, together with the autocorrelation function, ρ_{Lz} and power-spectra, P_{Lz}. The time series shows two types of vacillation behaviour *around* individual and *between* two fixed-points in phase-space. The power-spectrum P_{Lz} shows the signature of the former, with a peak occuring around 200-250 cycles. The expression of the latter is shown as enhanced power at low frequency (< 50 cycles). The other conspicuous feature within the spectra is the broadband exponential slope seen at frequencies > 50 cycles. The autocorrelation function ρ_{Lz} shows a weak drop in value < 2 time units, followed by a steep drop in value until 5 time units before, falling off more slowly at greater lags. The presence of the vacillations around the individual fixed points shows up as an oscillation in ρ_{Lz} with a period of 7 time units.

Our analysis demonstrates that the wintertime NAM at low frequencies ($1/\mathrm{f} > 36$ days) has more power than what would be expected from an extrapolation of the high-frequency exponential spectrum evident at high frequencies. These characteristics are also evident in the Lorenz-63 system and are in this case linked with the existence of fixed (saddle) points and a strange-attractor in phase space. Evidence of such dense points for the NAM

is debated and it is fair to say that there is currently no consensus on their existence or absence.

The excess variance at low frequencies can be interpreted as a definition of regimes in the time domain. In this definition, a regime is simply a longer than expected period (compared to some homogeneous in frequency null-hypothesis - e.g., a low order chaotic model) where the NAM persists around some value. This need not correspond to a fixed point of some lower order chaotic system, and so the "regimes" would not correspond to fixed patterns in real space or state space (or values, in the case of the NAM).

The presence of exponential spectra for high frequencies suggests that deterministic chaos dominates the high-frequency ($1/\mathrm{f} < 36$ days) NAM variability. This suggests one should exercise caution before interpreting the dynamics of the NAM as being stochastic in origin. Although such concepts can be useful in parameterising the long-range effects of chaotic variability, they can be misleading in diagnosing mechanisms for short-term and seasonal predictability.

Acknowledgments. We thank M. Baldwin for providing the NCEP derived NAM data for this project and also the thoughtful and constructive comments from two anonymous reviewers.

References

Ambaum, M., and B. Hoskins, The NAO troposphere-stratosphere connection, *J. Clim.*, *15*(14), 1969–1978, 2002.

Babloyantz, A., and A. Destexhe, Is the normal heart a periodic oscillator, *Biological Cybernetics*, *58*(3), 203–211, 1988.

Baldwin, M., and T. Dunkerton, Stratospheric harbingers of anomalous weather regimes, *Science*, *294*(5542), 581–584, 2001.

Barnes, E. A., and D. L. Hartmann, Testing a theory for the effect of latitude on the persistence of eddy-driven jets using CMIP3 simulations, *Geophys. Res. Lett.*, *37*, doi: 10.1029/2010GL044144, 2010.

Barnes, E. A., D. L. Hartmann, D. M. W. Frierson, and J. Kidston, Effect of latitude on the persistence of eddy-driven jets, *Geophys. Res. Lett.*, *37*, doi:10.1029/2010GL043199, 2010.

Bracewell, R., *The Fourier Transfor and its Applications*, McGraw-Hill, 1978.

Brandstater, A., and H. Swinney, Strange attractors in weakly turbulent couette-taylor flow, *Physical Review A*, *35*(5), 2207–2220, 1987.

Elhamdi, M., M. Gorman, and K. Robbins, Deterministic chaos in laminar premixed flames - experimental classification of chaotic dynamics, *Combustion Science and Technology*, *94*(1-6), 87–101, 1993.

Feldstein, S., The timescale, power spectra, and climate noise properties of teleconnection patterns, *J. Clim.*, *13*(24), 4430–4440, 2000.

Franzke, C., and T. Woollings, On the Persistence and Predictability Properties of North Atlantic Climate Variability, *JOURNAL OF CLIMATE*, *24*(2), 466–472, doi: 10.1175/2010JCLI3739.1, 2011.

Frisch, U., and R. Morf, Intermittency in non-linear dynamics and singularities at complex times, *Physical Review A*, *23*(5), 2673–2705, 1981.

Gerber, E., and G. Vallis, A Stochastic model for the spatial structure of annular patterns of variability and the North Atlantic Oscillation, *J. Clim.*, *18*(12), 2102–2118, 2005.

Gerber, E. P., and G. K. Vallis, Eddy-zonal flow interactions and the persistence of the zonal index, *J. Atmos. Sci.*, *64*(9), 3296–3311, doi:10.1175/JAS4006.1, 2007.

Hannachi, A., On the Origin of Planetary-Scale Extratropical Winter Circulation Regimes, *J. Atmos. Sci.*, *67*(5), 1382–1401, doi:10.1175/2009JAS3296.1, 2010.

Hartmann, D., and F. Lo, Wave-driven zonal flow vacillation in the Southern Hemisphere, *JOURNAL OF THE ATMOSPHERIC SCIENCES*, *55*(8), 1303–1315, 1998.

Hasselmann, K., Stochastic climate models part i. theory, *Tellus*, *28*(6), 473–485, doi:10.1111/j.2153-3490.1976.tb00696.x, 1976.

Keeley, S. P. E., R. T. Sutton, and L. C. Shaffrey, Does the North Atlantic Oscillation show unusual persistence on intraseasonal timescales?, *GEOPHYSICAL RESEARCH LETTERS*, *36*, doi:10.1029/2009GL040367, 2009.

Khintchine, A., Korrelationtheorie der stationären prozesse, *Math. Ann.*, *109*, 604–615, 1934.

Lorenz, E., Deterministic nonperiodic flow, *J. Atmos. Sci.*, *20*(2), 130–141, 1963.

Norton, W., Sensitivity of northern hemisphere surface climate to simulation of the stratospheric polar vortex, *Geophys. Res. Lett.*, *30*(12), doi:10.1029/2003GL016958, 2003.

Ohtomo, N., K. Tokiwano, Y. Tanaka, A. Sumi, S. Terachi, and H. Konno, Exponential characteristics of power spectral densities caused by chaotic phenomena, *Journal of the*

Physical Society of Japan, *64*(4), 1104–1113, 1995.

Pace, D. C., M. Shi, J. E. Maggs, G. J. Morales, and T. A. Carter, Exponential frequency spectrum in magnetized plasmas, *Physical Review Letters*, *101*(8), doi: 10.1103/PhysRevLett.101.085001, 2008.

Sigeti, D., Survival of deterministic dynamics in the presence of noise and the exponential decay of power spectra at high-frequency, *Physical Review E*, *52*(3, Part A), 2443–2457, 1995a.

Sigeti, D., Exponential decay of power spectra at high-frequency and positive lyapunov exponents, *Physica D*, *82*(1-2), 136–153, 1995b.

Sigeti, D., and W. Horsthemke, High-frequency power spectra for systems subject to noise, *Physical Review A*, *35*(5), 2276–2282, 1987.

Stephenson, D., V. Pavan, and R. Bojariu, Is the North Atlantic Oscillation a random walk?, *Int. J. Climatol.*, *20*(1), 1–18, 2000.

Trenberth, K. E., Some effects of finite-sample size and persistence on meteorological statistics .1. autocorrelations, *Mon. Wea. Rev.*, *112*(12), 2359–2368, 1984.

Vallis, G., E. Gerber, P. Kushner, and B. Cash, A mechanism and simple dynamical model of the North Atlantic Oscillation and annular modes, *J. Atmos. Sci.*, *61*(3), 264–280, 2004.

Wiener, N., Generalised harmonic analysis, *Acta Math.*, *55*, 117–258, 1930.

Woollings, T., B. Hoskins, M. Blackburn, and P. Berrisford, A new Rossby wave-breaking interpretation of the North Atlantic Oscillation, *J. Atmos. Sci.*, *65*(2), 609–626, doi: 10.1175/2007JAS2347.1, 2008.

Woollings, T., A. Hannachi, B. Hoskins, and A. Turner, A Regime View of the North Atlantic Oscillation and Its Response to Anthropogenic Forcing, *J. Clim.*, *23*(6), 1291–1307, doi:10.1175/2009JCLI3087.1, 2010.

Figure 1. The filter (top) used to sift NCEP NAM time series for the calculation of time-of-year autocorrelation and its corresponding Fourier transform (bottom). See (2) and text for details.

Figure 2. Representative NCEP Power spectra for summer (red) and winter (blue). Lorentzian fits are made at low frequencies ($0 < \omega < \omega_c$) for both summer ($\omega_c = 30 \times 2\pi\,\mathrm{yr}^{-1}$) and winter ($\omega_c = 10 \times 2\pi\,\mathrm{yr}^{-1}$). Exponential fits are made for $\omega > \omega_c$. Also shown are lorentzian fits extending over all frequencies, characteristic of AR1 processes (thick lines). For clarity a spectral smoothing is made using a spectral window of width $1 \times 2\pi\,\mathrm{yr}^{-1}$.

Figure 3. Representative NCEP autocorrelations for summer (red) and winter (blue). Observed values (dashed) are compared with the retrieved estimates of ρ_{fit} (thick) following inversion of P_{fit} using (4).

Figure 4. A numerical integration of the Lorenz-63 system showing (from top): timeseries, power-spectra and autocorrelation function. The time unit scale has been adjusted for comparison with previous results. Units are otherwise arbitrary.

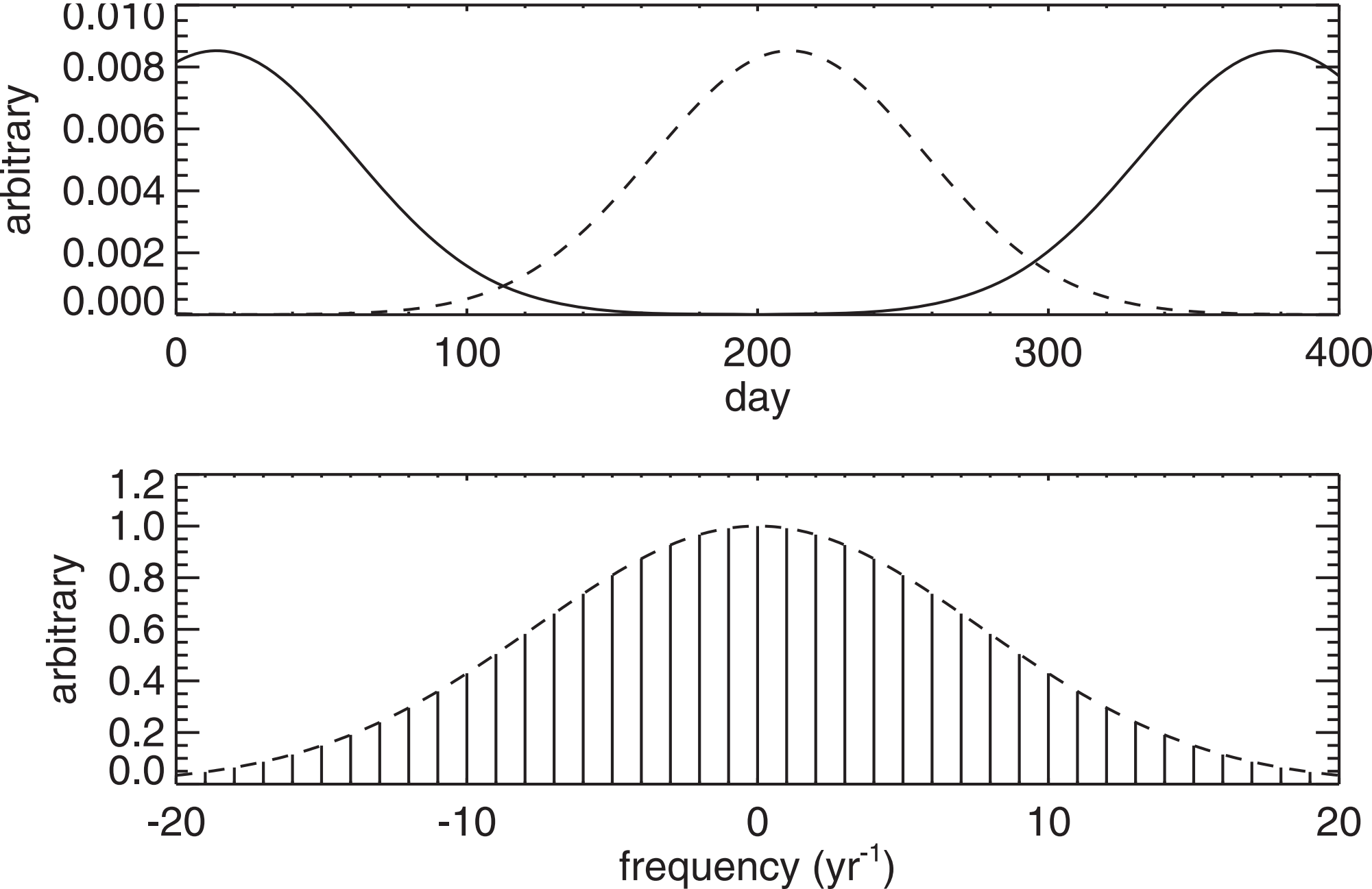
0.010
0.008
0.006
0.004
0.002
0.000
arbitrary
0
100
200
300
400
day
1.2
1.0
0.8
0.6
0.4
0.2
0.0
arbitrary
-20
-10
0
10
20
frequency (yr-1)

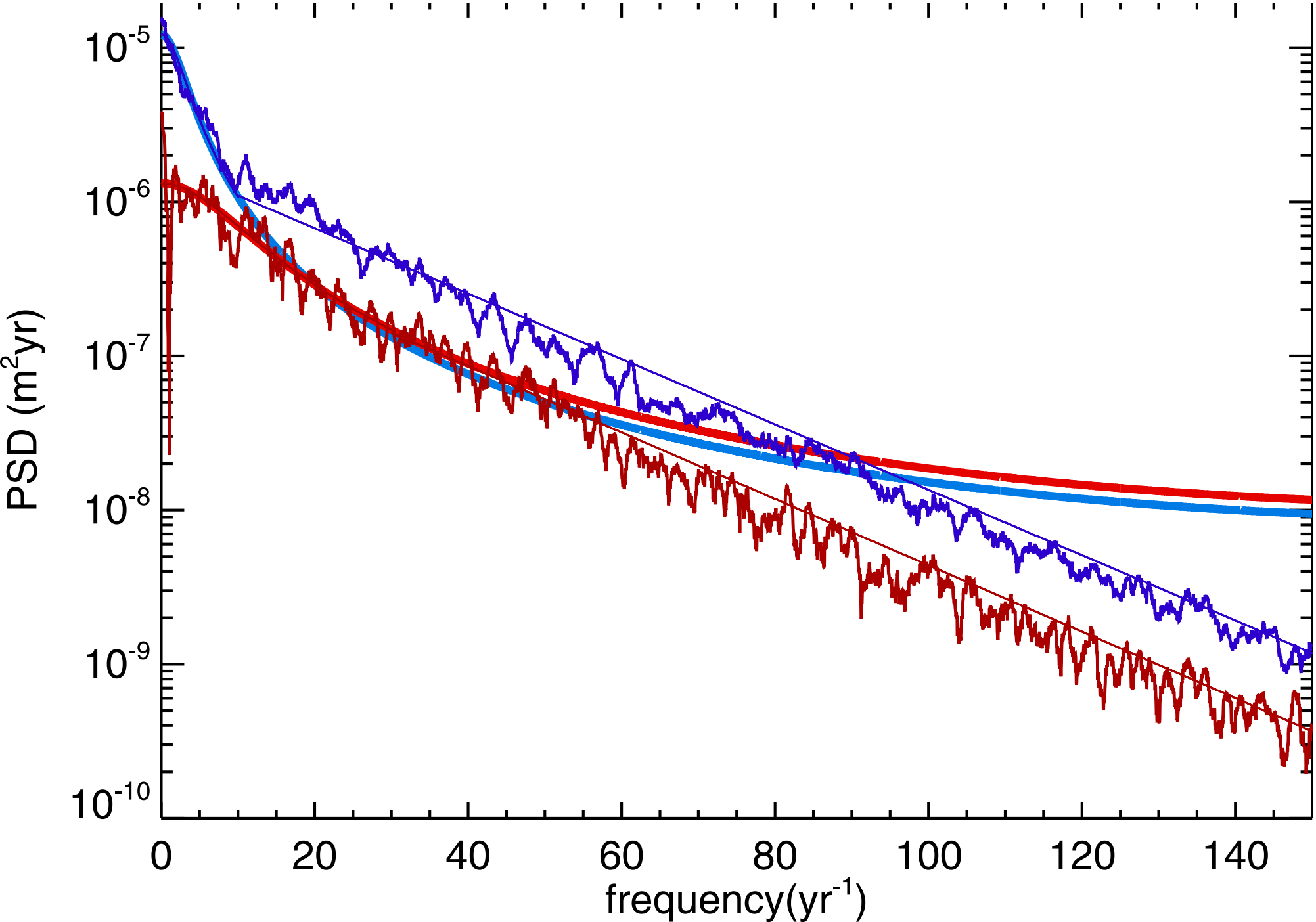
PSD (m²yr)
10⁻⁵
10⁻⁶
10⁻⁷
10⁻⁸
10⁻⁹
10⁻¹⁰
0
20
40
60
80
100
120
140
frequency(yr⁻¹)

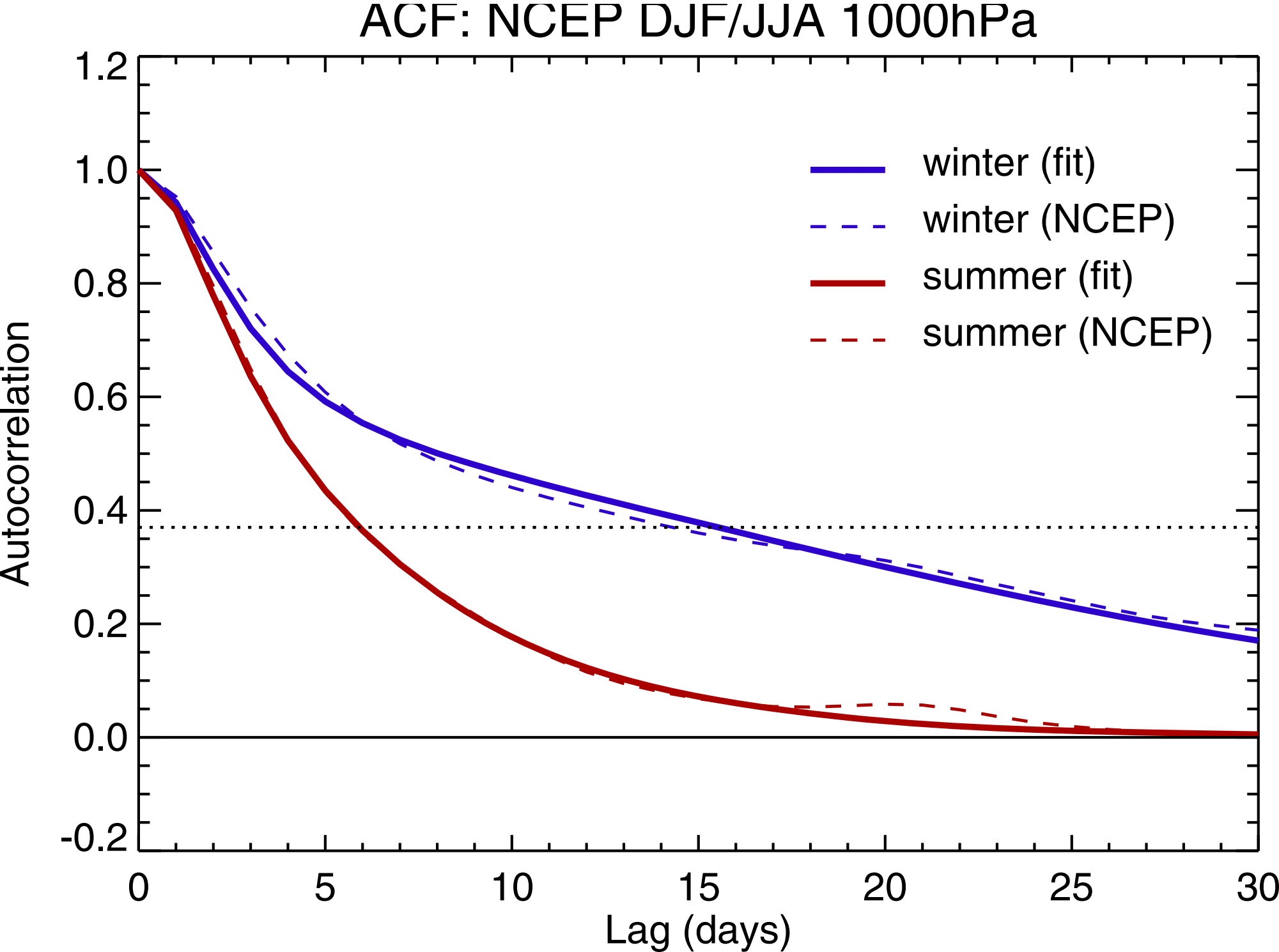
ACF: NCEP DJF/JJA 1000hPa
Autocorrelation
Lag (days)
1.2
1.0
0.8
0.6
0.4
0.2
0.0
-0.2
0
5
10
15
20
25
30
winter (fit)
winter (NCEP)
summer (fit)
summer (NCEP)

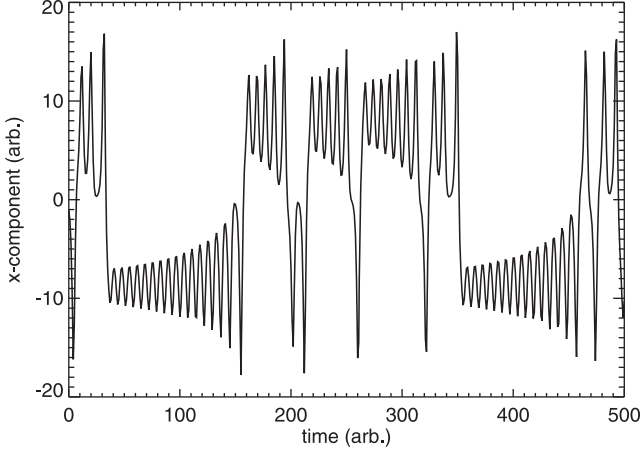
x-component (arb.)
time (arb.)

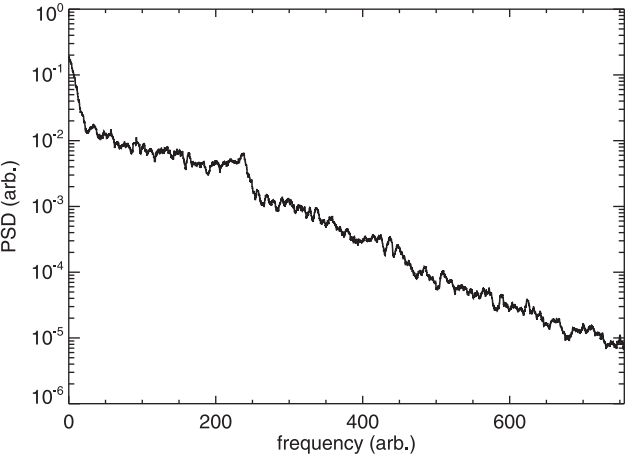
PSD (arb.)
frequency (arb.)

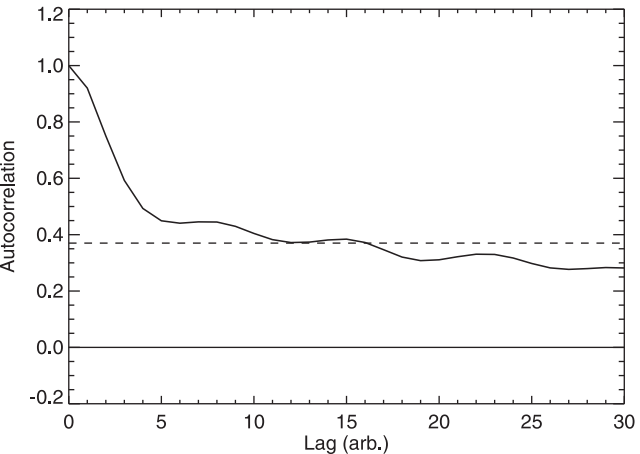
Autocorrelation
Lag (arb.)